

TetraCobalt-Polyoxometalate Catalysts for Water Oxidation: Key Mechanistic Details

Joaquín Soriano-López,^{†,§} Djamaladdin G. Musaev,^{*,†} Craig Hill,[‡]

José Ramón Galán-Mascarós,[†] Jorge J. Carbó,^{*,§} Josep M. Poblet^{*,§}

[†] Institute of Chemical Research of Catalonia (ICIQ), Av. Països Catalans 16, E-43007 Tarragona, Spain

[‡] Emerson Center for Scientific Computation and Department of Chemistry, Emory University, 1515 Dickey Dr., Atlanta, Georgia, 30322, United States of America

[§] Departament de Química Física i Inorgànica, Universitat Rovira i Virgili, Marcel·lí Domingo 1, 43007 Tarragona, Spain

ABSTRACT: A mechanism of water oxidation catalyzed by the carbon-free tetra-Co containing polyoxometalates $[\text{Co}_4(\text{H}_2\text{O})_2(\text{PW}_9\text{O}_{34})_2]^{10-}$ (PCo_4) and $[\text{Co}_4(\text{H}_2\text{O})_2(\text{VW}_9\text{O}_{34})_2]^{10-}$ (VCo_4) is elucidated by DFT calculations. Computational analysis for PCo_4 suggests that a first PCET step may proceed via a sequential electron-then-proton transfer (ET+PT) pathway and leads to one electron oxidized species S_1 (POM-Co^{III}-OH). In contrast, the second PCET, which controls the potential required to form POM-Co^{III}-O[•] active species S_2 is clearly a *concerted* process. The overall $\text{S}_0 \rightarrow \text{S}_2$ transformation is estimated to require less than 1.48 V and 1.62 V applied potential at pH=8 for PCo_4 and VCo_4 anions, respectively. At operando conditions, with the presence of a buffer and with an applied potential above the threshold potential the two H-atom removal could take place via concerted pathways. These steps represent rapid pre-equilibria before the rate determining step, which corresponds to the O-O bond formation. The key *chemical* step occurs via nucleophilic attack of an external water molecule to intermediate S_2 . We assume that this step governs the *kinetics* of the reaction. Comparison of the calculated energetics and electronic structures of intermediate species in the PCo_4 and VCo_4 catalyzed water oxidation cycle shows that coupling of d orbitals of V and Co atoms in VCo_4 increases the oxidation potential of the Co-center. The orbital coupling is also responsible for the higher catalytic activity of VCo_4 because it increases the electrophilicity of Co^{III}-O[•] moiety in the key S_2 species.

INTRODUCTION

Natural photosynthesis in higher green plants involves complex reactions that use solar energy to oxidize H_2O into O_2 within the Photosystem II (PSII) and generates reducing equivalents, which are used by Photosystem I (PSI) to reduce CO_2 to carbohydrates. The aim of the artificial photosynthesis is the harvesting of the solar energy and its storage in chemical bonds, by means of water splitting obtaining fuels and oxygen.[1, 2] One of the bottlenecks of artificial photosynthesis is the design of a efficient water oxidation catalyst (WOC), which has to be fast, inexpensive, robust, and has to enable the water oxidation close to the thermodynamic potential working in environmentally friendly conditions.[3]

Recently, numerous homogeneous molecular water oxidation catalysts have been reported,[4-19] among which carbon-free polyoxometalate (POM)

complexes are promising. [20, 21] These complexes act as WOCs in both homogeneous and heterogeneous conditions,[22, 23] and yet, are all-inorganic species with high stability towards oxidative degradation.[24, 25]

The first reported POM showing effective water oxidation activity was the $[\text{Ru}_4\text{O}_4(\text{OH})_2(\text{H}_2\text{O})_4(\gamma\text{-SiW}_{10}\text{O}_{36})_2]^{10-}$ complex.[26-31] However, recently POMs with earth-abundant metals showing superior water oxidation activity were foci of chemical and catalytic sciences.

In 2010, Hill and co-workers have reported the first Co-containing polyoxometalate WOC, $[\text{Co}_4(\text{H}_2\text{O})_2(\text{PW}_9\text{O}_{34})_2]^{10-}$ (PCo_4).[32, 33] This complex contains a tetracobalt oxide core that is sandwiched by two lacunary PW_9O_{34} polytungstate cages with phosphorus atoms inside the cage (see Figure 1).

A higher nuclearity Co-containing POM, the nonanuclear $[\text{Co}_9(\text{H}_2\text{O})_6(\text{OH})_3(\text{HPO}_4)_2(\text{PW}_9\text{O}_{34})_3]^{16-}$ (PCo_9) cluster, has also exhibited WOC performance both in homogeneous conditions[34] and in the solid state, when incorporated into a carbon paste modified electrodes. This complex shows high oxygen evolution rates in a wide range of pH.[35] The replacement of P^{V} in PCo_4 with V^{V} leads to $[\text{Co}_4(\text{H}_2\text{O})_2(\text{VW}_9\text{O}_{34})_2]^{10-}$ (VCo_4), which is about 20 times faster than the phosphorus analog PCo_4 using $[\text{Ru}(\text{bpy})_3]^{3+}$ as chemical oxidant under dark conditions at pH=9. Besides their intrinsic interest, Co-containing POMs can be viewed as discrete molecular models of extended heterogeneous cobalt oxide catalyst due to their apparent structural analogy. The much studied Kanan-Nocera heterogeneous cobalt oxide phosphate WOC (CoP_i)[36] has some structural features in common with these poly-cobalt POMs.

Atomistic level understanding of mechanisms and governing factors of water oxidation by transition metal catalysts is expected to advance on the design of more efficient, stable, fast and cost-effective WOCs. The mechanism of water oxidation catalyzed by Ru-based systems has been subject of extensive studies.[37-51] However, the mechanism and governing factors of the Co-containing catalysts still remain elusive, and computational approaches are expected to play a crucial role in solution of these problems. Recent mechanistic studies on heterogeneous cobalt oxide catalysts have focused on various cluster and periodic model systems of the cobalt phosphate WOC (CoP_i)[52-57], as well as on recently synthesized homogeneous cubane-type WOCs.[58]

In general, these studies have shown that water oxidation by CoP_i is initiated by successive Proton Coupled Electron Transfer (PCET) events leading to the formation of the active Co^{IV} -oxo or Co^{III} -oxyl species, which is involved in the formation of the O–O bond. Two different mechanisms for the O–O formation have been proposed: i) “water nucleophilic attack” (WNA) mechanism, involving intermolecular nucleophilic attack of external water to the electrophilic Co^{IV} -oxo or Co^{III} -oxyl species,[53] and ii) “direct O–O coupling” mechanism proceeding via intramolecular direct coupling of two Co^{IV} -oxo sites.[52] These initial discrepancies were later attributed to the structural differences in the models used.[59]

Here, we elucidate mechanism of water oxidation by the sandwich species PCo_4 and VCo_4 , which have been extensively studied experimentally. Because of bulkiness and structural stability of these Co_4 -POM anions[32-34] one can eliminate the direct intermolecular O–O bond formation mechanism. Therefore, in the present paper, we only investigate in detail by computational means the key steps leading to the formation of the active Co^{IV} -oxo or Co^{III} -oxyl species, and WNA to O₂ bond formation mechanism of the water oxidation by the tetra-Co-containing POM catalysts.

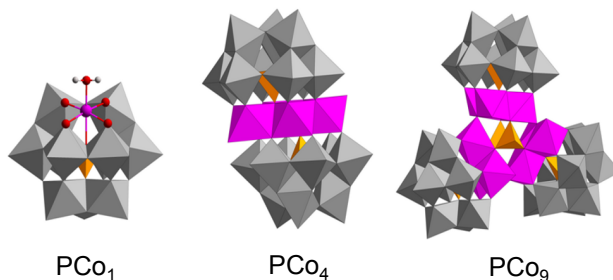


Figure 1. Polyhedral representation of the $[\text{Co}(\text{H}_2\text{O})\text{PW}_{11}\text{O}_{39}]^{5-}$ (PCo_1), $[\text{Co}_4(\text{H}_2\text{O})_2(\text{PW}_9\text{O}_{34})_2]^{10-}$ (PCo_4) and $[\text{Co}_9(\text{H}_2\text{O})_6(\text{OH})_3(\text{HPO}_4)_2(\text{PW}_9\text{O}_{34})_3]^{16-}$ (PCo_9) polytungstate anions.

RESULTS AND DISCUSSION

1. Electronic and Structural Properties of the PCo_4 and VCo_4 Catalysts. Previous experimental studies have shown[32, 33, 60] that at the resting stages of $[\text{Co}_4(\text{H}_2\text{O})_2(\text{PW}_9\text{O}_{34})_2]^{10-}$ (PCo_4) and $[\text{Co}_4(\text{H}_2\text{O})_2(\text{VW}_9\text{O}_{34})_2]^{10-}$ (VCo_4) anions all four Co atoms are in their 2+ oxidation states with a formal high-spin d^7 electron configuration and three unpaired electrons. From these three unpaired electrons two occupy an e_g -like and one a t_{2g} -like orbitals. In the presented computational (DFT) work, we do not analyze the magnetic coupling among the four $\text{Co}(\text{II}, d^7)$ centers. Thus, we discuss only the high-spin electronic state of the S_0 species with twelve (three per Co-center) unpaired electrons, in which, for simplicity of our analysis, we fixed C_{2h} symmetry in both PCo_4 and VCo_4 . Furthermore, in this ground state (S_0) of PCo_4 and VCo_4 , the water ligand is linked to the external Co^{II} centers with a relatively long Co–OH₂ bond length (2.24 Å), and adopted an orientation to accentuate the interactions between the hydrogen atoms and the terminal oxo sites of the POM (with O–H...O=W distance of ~2.01 Å, see Figure 2).

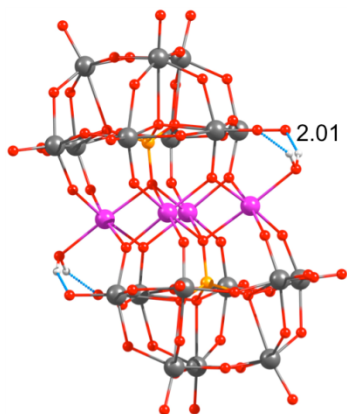


Figure 2. Ball and stick representation for PCo_4 .

2. Water oxidation by the PCo_4 anion.

A. Initial steps. Water oxidation is usually catalyzed by using either photo-induced (utilizing organic compounds as electron sinks) or electrochemical (applying a potential to oxidize water) approaches. Below, we focus on the issues related to the electrochemical water oxidation. In the studied process, the oxidation steps of the reactive center are controlled by the applied potential, while the chemical steps of the reaction depend on O–H bond cleavage and O–O bond formation energies, and dictate the kinetics of the reaction. In other words, in order to initiate the studied water oxidation it is necessary to apply a *threshold* potential, while the following bond formation/cleavage steps of the reaction do not depend on this applied potential. Keeping in mind these two control factors, along this article we present our results in V or $\text{kcal}\cdot\text{mol}^{-1}$ (or eV) depending if we are referring to the electrochemically or kinetically controlled steps, respectively.

Existing experiments show that most of the catalytic processes utilizing cobalt-containing POMs occur in neutral or basic media (often at $\text{pH}=8$).^[22-25] Therefore, we focus the discussion of our results considering that the Co_4 -catalyzed water oxidation occurs at $\text{pH}=8$. Here, we estimate the effect of pH on a $\text{S}_i \rightarrow \text{S}_j$ transformation by using standard Nernst eq. 2, in which we have assumed that S_i and S_j species have identical concentrations.

Taking as a starting point the mechanism proposed for single-site cobalt^[61-63] and ruthenium^[37-44] catalysts, we first analyze the solution speciation of the S_0 species at $\text{pH}=8$. Casey and co-workers^[64] studied the rates of water exchange of PCo_4 by means of spectroscopic and potentiometric techniques, concluding that the pK_a for the first deprotonation of the water ligand [$\text{S}_0(\text{Co}^{\text{II}}-\text{OH}_2) \rightarrow \text{S}_0'(\text{Co}^{\text{II}}-\text{OH})$] would be close to 8.

Shortly after, Ivanović-Burmazović et al.^[65] also studied the water exchange reactivity and stability of PCo_4 in the 6 to 10 pH range, which is the catalytically relevant pH region, employing ^{17}O -NMR spectroscopy and ultrahigh-resolution electrospray ionization mass spectrometry. In that work, it was found no evidence of Co–hydroxo or Co–oxo species formation in the studied pH range ($\text{pH}=6\text{-}10$). Hence, authors concluded that the pK_a for the first deprotonation of PCo_4 should be higher than 10. Note that the POM is unstable above $\text{pH}=10$.^[25] Despite experimental evidences, we decided to compute the deprotonation of S_0 species in order to confirm that the pK_a value could be higher than 10, and consequently, that the true nature of the catalyst corresponds to the Co(II)-aqua species S_0 . For the [$\text{S}_0(\text{Co}^{\text{II}}-\text{OH}_2) \rightarrow \text{S}_0'(\text{Co}^{\text{II}}-\text{OH})$] step we have estimated a pK_a value of 19.7 and an endergonic free energy of $+16.1 \text{ kcal}\cdot\text{mol}^{-1}$ at $\text{pH}=8$ (Figure 4). Deviations of computed pK_a values with respect to experimental ones can be significant as it has already been pointed out. Hence discrepancies between experimental and computed pK_a of 5 units are not unusual,^[39] where 1 pK_a unit represents 60 meV, $1.38 \text{ kcal}\cdot\text{mol}^{-1}$. Reported experimental data and our present calculations strongly suggest that the pK_a for the first proton removal step should be higher than 10. Thus, at $\text{pH}=8$, where catalytic experiments are performed, the predominant species existing in solution is $\text{S}_0(\text{Co}^{\text{II}}-\text{OH}_2)$, whereas the concentration of $\text{S}_0'(\text{Co}^{\text{II}}-\text{OH})$ species should be negligible.

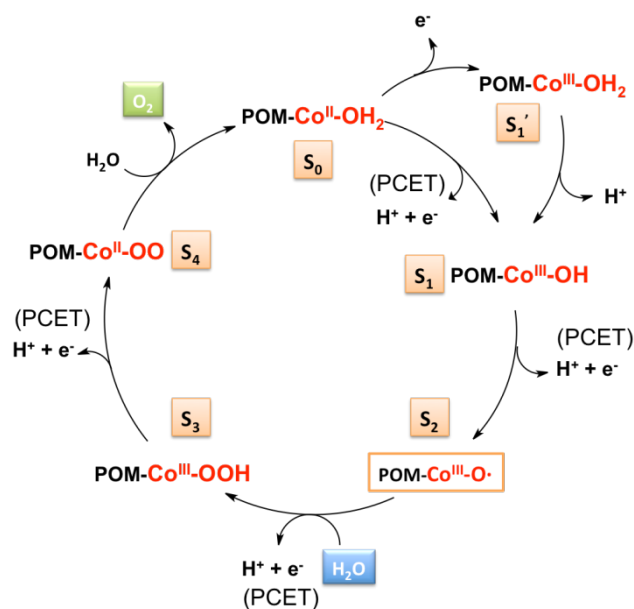


Figure 3. Schematic presentation of the water oxidation single-site catalyst mechanism using cobalt-containing polyoxometalates.

Thus, we analyze each step of the PCo_4 -catalyzed water oxidation cycle at $\text{pH}=8$ starting from the $\text{S}_0(\text{Co}^{\text{II}}-\text{OH}_2)$ species (see Figure 3). According to this mechanism, the first step of the overall process is the H-atom removal from the coordinated water molecule of the resting $\text{Co}^{\text{II}}-\text{OH}_2$ (S_0) state of the system. This step leads to the $\text{Co}^{\text{III}}-\text{OH}$ species (S_1) with one-electron oxidized Co-center (*i.e.* from Co^{II} to Co^{III}) and deprotonated water (*i.e.* OH) ligand. In the next step, the S_1 species transforms to the $\text{Co}^{\text{III}}-\text{oxyl}$ species (S_2) with one electron oxidized and deprotonated oxyl ligand. Both these steps of the reaction, in general, could occur via either proton-coupled electron transfer (PCET), sequential proton-then-electron transfer (PT+ET) or sequential electron-then-proton transfer (ET+PT) pathways; hence, we analyze the three of them for each step. The computed free energies are shown in Figure 4. The vertical steps in the square diagram represent one-electron oxidation reactions, the free energies of which are expressed as standard reduction potentials. Horizontal steps represent acid-base equilibria, the free energies of which may have associated a pK_a .^[18] Finally, diagonal steps represent concerted PCET steps. Hence, the first H-atom removal from the coordinated water molecule, *i.e.* the $\text{S}_0 \rightarrow \text{S}_1$ transition, via the PCET pathway requires 1.51 V potential *vs* to NHE. As already mentioned, the PT+ET pathway is unlikely in this step, since deprotonation of the water ligand in the S_0 species is thermodynamically unfavorable and it would need strong basic conditions ($\text{pH}>10$) where PCo_4 is unstable. The same step of the reaction proceeding via the sequential ET+PT requires lower applied potential (1.27 V for $\text{S}_0 \rightarrow \text{S}_1'$) than the concerted PCET (1.51 V). Nevertheless, the free energy for the subsequent deprotonation ($\text{S}_1' \rightarrow \text{S}_1$) step is slightly endergonic $+5.5 \text{ kcal}\cdot\text{mol}^{-1}$ (+0.24 eV), and consequently, the ET+PT process requires additional chemical *thermal* energy in order for the reaction to proceed, slowing down the overall kinetics of the reaction. It is worthy to point out that in the present model bulk water is considered the proton acceptor in the PT events (as well as in the PCET events). This assumption implies that the computed free energies might be viewed as upper limit energies, since actually buffer (phosphate, borate, etc.) may act as the proton acceptor during experimental conditions. In other words, whenever the proton acceptor is a stronger base than bulk water the free energies required to proceed through the deprotonation step will be lower than the computed ones. Therefore, at the reaction conditions where always a buffer is used and the potential is somewhat greater than the minimum

required, concerted and sequential paths are competitive.

Once the reaction reaches the $\text{S}_1(\text{Co}^{\text{III}}-\text{OH})$ state, the second oxidation process (*i.e.* $\text{S}_1 \rightarrow \text{S}_2$) proceeds. Following the same procedure, we computed again PCET [$\text{S}_1(\text{Co}^{\text{III}}-\text{OH}) \rightarrow \text{S}_2(\text{Co}^{\text{III}}-\text{O}^\bullet)$], PT+ET [$\text{S}_1(\text{Co}^{\text{III}}-\text{OH}) \rightarrow \text{S}_1''(\text{Co}^{\text{III}}-\text{O}) \rightarrow \text{S}_2(\text{Co}^{\text{III}}-\text{O}^\bullet)$] and ET+PT [$\text{S}_1(\text{Co}^{\text{III}}-\text{OH}) \rightarrow \text{S}_2'(\text{Co}^{\text{III}}-\text{OH}^\bullet) \rightarrow \text{S}_2(\text{Co}^{\text{III}}-\text{O}^\bullet)$] pathways. We found that the H-atom removal from the OH-ligand via the concerted PCET pathway requires an applied potential of 1.48 V. Considering the sequential proton-then-electron transfer pathway (PT+ET), deprotonation of $\text{S}_1(\text{Co}^{\text{III}}-\text{OH})$ species requires an energy as high as $+45.8 \text{ kcal}\cdot\text{mol}^{-1}$ (1.99 eV). Finally, the sequential electron-then-proton transfer needs an applied potential of 2.59 V for the ET event. Thus, the two sequential pathways require rather high energies to be initiated, and we can conclude that the second H-atom removal occurs preferably via a concerted PCET event, where the electron and the proton are transferred in one step from the OH-ligand [$\text{S}_1(\text{Co}^{\text{III}}-\text{OH}) \rightarrow \text{S}_2(\text{Co}^{\text{III}}-\text{O}^\bullet)$], with an applied potential of 1.48 V.

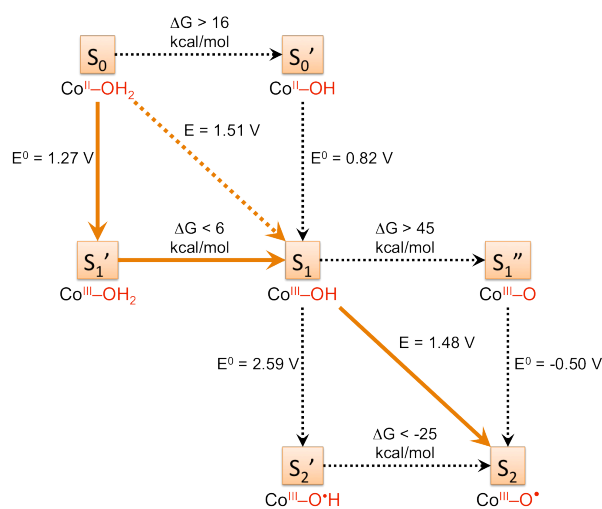


Figure 4. Schematic presentation of the PCET, PT+ET, and ET+PT events for PCo_4 WOC at $\text{pH}=8$. Potentials are given in V, whereas values associated to deprotonation steps are given in kcal/mol. The orange dashed line in the first concerted PCET indicates that the process may become competitive with the sequential ET+PT at $E_{\text{app}} > 1.51 \text{ V}$.

In electrochemical catalysis the potentials are not additives as those are in the chemical catalysis. Therefore, one may conclude that in the electrochemical conditions the formation of the active species $\text{S}_2(\text{Co}^{\text{III}}-\text{O}^\bullet)$ will require an applied potential of about 1.5 V at $\text{pH}=8$. At this potential the concerted PCET of the first H-atom removal ($\text{S}_0 \rightarrow \text{S}_1$) is feasible and we cannot discard that it competes with the sequential ET+PT occurring at

lower potential. These findings are consistent with the previous electrochemical analysis of PCo_4 . Indeed, previous cyclic voltammetry experiments shown an onset potential of 1.46 V vs NHE at pH=7.8 for water oxidation using PCo_4 as a catalyst.[66]

Despite the complexity presented above, we still can draw the following conclusions from the presented computational findings: 1) removal of the first electron (*i.e.* oxidation of Co^{II} to Co^{III} ($\text{S}_0 \rightarrow \text{S}_1'$)) is less energetically demanding than the removal of the second electron (*i.e.* ($\text{S}_1 \rightarrow \text{S}_2'$)); 2) the first oxidation step does not necessarily occur coupled to a proton transfer, while the second oxidation is a concerted PCET event; and 3) the potential required for the overall two-electron redox reaction is determined by the second oxidation step, that is the formation of the *active species* (S_2).

Close examination of geometry parameters of various intermediate oxidation states of PCo_4 shows that the change of external Co-O bond distance (it is established that in the sandwich POMs the external TM-OH₂ sites are reactive sites[67]) along the water oxidation cycle is consistent with the nature of the oxidation events. Indeed, oxidation of the cobalt center [*i.e.* $\text{S}_0(\text{Co}^{\text{II}}\text{-OH}_2) \rightarrow \text{S}_1'(\text{Co}^{\text{III}}\text{-OH}_2)$] shortens the Co-OH₂ bond distance from 2.24 Å to 1.96 Å. The following loss of the first [*i.e.* $\text{S}_1'(\text{Co}^{\text{III}}\text{-OH}_2) \rightarrow \text{S}_1(\text{Co}^{\text{III}}\text{-OH})$] and the second [*i.e.* $\text{S}_1(\text{Co}^{\text{III}}\text{-OH}) \rightarrow \text{S}_2(\text{Co}^{\text{III}}\text{-O}^{\bullet})$] proton further reduces the calculated Co-O bond distance to 1.82 Å and 1.76 Å, respectively (see Table 2).

Aforementioned geometry changes are also consistent with the nature of the frontiers orbitals

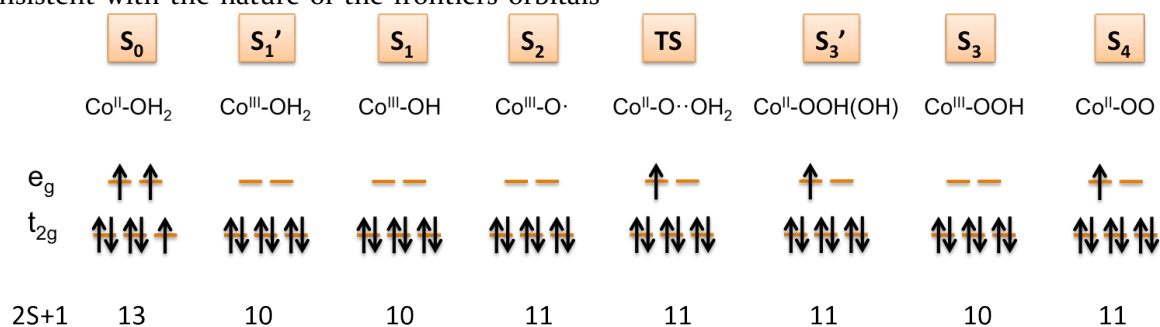


Figure 6. Unpaired spin distribution in the active Co sites of different species involved in the PCo_4 catalyzed water oxidation mechanism.

Table 1. Computed Values for Each Step of the PCo_4 - and VCo_4 -catalyzed Water Oxidation Cycles at pH=8.

POM	$\text{S}_0 \rightarrow \text{S}_1'$ ^{a)} (V)	$\text{S}_1' \rightarrow \text{S}_1$ ^{b)} (eV)	$\text{S}_1 \rightarrow \text{S}_2$ ^{a)} (V)	$\text{S}_2 \rightarrow \text{TS}$ ^{c)} (eV)	$\text{S}_2 \rightarrow \text{S}_3'$ ^{c)} (eV)	$\text{S}_3' \rightarrow \text{S}_3$ ^{a)} (V)	$\text{S}_3 \rightarrow \text{S}_4$ ^{a)} (V)
PCo_4 ^{d)}	+1.27	+0.24	+1.48	+0.99	+0.22	+0.26	+0.05
VCo_4 ^{d)}	+1.58	+0.32	+1.62	+0.73	-0.11	+0.42	+0.07

a) For the electrochemical steps the potentials are given in V versus NHE; b) Values corresponding to the deprotonation step (eV); c) Energy values for the activation barrier of the transition state are given in eV. d) Values in bold represent the threshold potentials and energy barriers to overcome for PCo_4 and VCo_4 at pH=8.

of the intermediate species. Indeed, as seen in Figure 5, the contribution of ligand p(O) orbital to the HOMO is significant in S_1 species and, consequently, the next oxidation event is expected to be hydrogen removal from OH-fragment that leads to the Co^{III} -oxyl species S_2 ($\text{POM-Co}^{\text{III}}\text{-O}^{\bullet}$). Consistently, in S_2 species the calculated spin population of oxyl-center is 1.00 |e| (see Figures 5 and 6). One should mention that the oxidation of $\text{Co}^{\text{III}}\text{-OH}$ leads to the $\text{Co}^{\text{III}}\text{-O}^{\bullet}$ species rather than the $\text{Co}^{\text{IV}}\text{-O}$ unit. A similar result was previously reported for cobalt oxide cubane systems[52] and single-site Co-corrole catalysts.[61-63] More recently, DFT and CASSCF studies of the Co derivatives of POMs also revealed that the formation of a Co^{IV} species is energetically unfavorable.[68] Similarly, for Ru-containing POMs, it was suggested that the Ru^{VI} -oxo groups are formally closer to being Ru^{V} -oxyl radicals. [45]

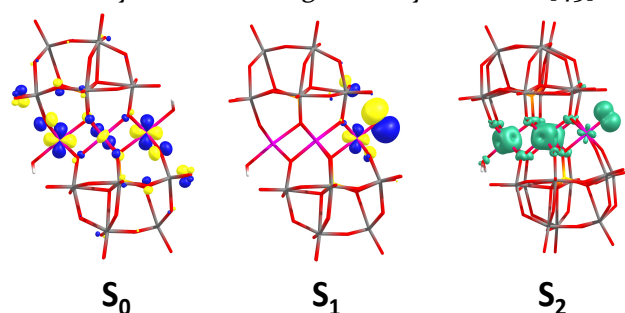


Figure 5. The HOMOs and the spin densities of several species of the PCo_4 -catalyzed water oxidation cycle.

Table 2. The Calculated Co-O Bond Distances (in Å) and Unpaired Mulliken Spin Densities (in |e|) of the Co and “active” O-centers for the Different Intermediate Species (S_i) of the PCo_4 - and VCo_4 -catalyzed Water Oxidation Cycles.^{a)}

		S_0	S_1'	S_1	S_2	TS	S_3'	S_3	S_4
	POM	$\text{Co}^{\text{II}}\text{-OH}_2$	$\text{Co}^{\text{III}}\text{-OH}_2$	$\text{Co}^{\text{III}}\text{-OH}$	$\text{Co}^{\text{III}}\text{-O}^{\cdot}$	$\text{Co}^{\text{II}}\text{-O}+\text{H}_2\text{O}$	$\text{Co}^{\text{II}}\text{-OOH(OH)}$	$\text{Co}^{\text{III}}\text{-OOH}$	$\text{Co}^{\text{II}}\text{-OO}$
$d(\text{Co-O}_i)$	PCo_4	2.240	1.956	1.820	1.760	1.730	1.876	1.832	2.060
	VCo_4	2.220	1.968	1.821	1.761	1.734	1.867	1.833	2.013
$d(\text{Co-O}_e)$	PCo_4	2.240	1.969	2.100	2.100	2.070	2.097	2.106	2.164
	VCo_4	2.150	1.938	2.064	2.062	2.018	2.066	2.062	2.117
$\rho(\text{Co})$	PCo_4	2.73	0.00	0.00	-0.04	1.15	1.01	0.01	0.79
	VCo_4	2.78	0.00	-0.01	-0.06	1.35	1.03	-0.01	0.71
$\rho(\text{O})$	PCo_4	0.03	0.00	-0.01	1.00	-0.14 (-0.10)	-0.06 (-0.01)	-0.01 (0.00)	0.09 (0.15)
	VCo_4	0.03	0.00	0.01	1.01	-0.26 (-0.17)	-0.08 (-0.01)	0.00 (0.00)	0.11 (0.21)

a) Values in parentheses are for the second oxygen atom after the O-O bond formation.

B. The O-O bond formation: Nucleophilic attack of water to the $\text{Co}^{\text{III}}\text{-oxyl}$ (S_2) species.

Once the active cobalt-oxyl species (S_2) is formed, next step of the water oxidation by $\text{Co}_4\text{-POM}$ catalyst is the O-O bond formation, which, as we mentioned above, is expected to occur via the WNA mechanism. This process, which is initiated by the nucleophilic attack of an “external” water molecule to the $\text{Co}^{\text{III}}\text{-oxyl}$ intermediate S_2 , will be followed by two more PCET events, and will release molecular O_2 . Once again, we rule out the intramolecular formation of O-O bond from two Co-oxyl groups in the same POM because of large distance between these two oxo atoms (>9.6 Å).

As seen in Figure 6, nucleophilic attack of water to intermediate $S_2(\text{Co}^{\text{III}}\text{-O}^{\cdot})$ yields $[\text{Co}^{\text{II}}(\text{OOH})\text{Co}_3^{\text{II}}(\text{H}_2\text{O})(\text{PW}_9\text{O}_{34})_2\text{H}]^{10-}$ (S_3') species, where one of the protons of coordinated (external) water is transferred to a basic oxygen atom of the POM in a concerted manner, as shown in Figure 7. Since oxygens of the Co-O-W bridges are the most basic ones, they are the most likely to be protonated.[69-72] The free energy barrier for the water HO-H bond activation is calculated to be 0.99 eV at the transition state TS (see Table 1 and Figure 8). We note that the LUMO+1 of the active S_2 ($\text{Co}^{\text{III}}\text{-O}^{\cdot}$) species, has a Co-O π^* -antibonding character (Figure 7) and is significantly polarized toward the oxyl ligand; this clearly favors the nucleophilic attack of a water molecule. [7, 37, 44, 46] The following PCET event from species S_3 requires an applied potential of 0.26 V, and yields the intermediate $[\text{Co}^{\text{III}}(\text{OOH})\text{Co}_3^{\text{II}}(\text{H}_2\text{O})(\text{PW}_9\text{O}_{34})_2]^{10-}$ (S_3), the ground state of which has nine unpaired electrons (three electrons on each Co^{II} centers and a low-spin Co^{III} ion) (see Figure 6).

The last PCET event requires a relatively low energy of 0.05 V, and leads to the formation of the $\text{Co}^{\text{II}}\text{-OO}$ (S_4) species with ten unpaired electrons, only one of which is localized in the reactive cobalt

center. The last step involves the molecular oxygen released from species S_4 upon coordination of another water molecule that regenerates the catalyst. Thus, based on above presented data, if the $\text{Co}^{\text{III}}\text{-O}^{\cdot}$ species (S_2) has been formed (via either chemically or electrochemically or photochemically), then the following O-O bond formation would occur with less energy demand.

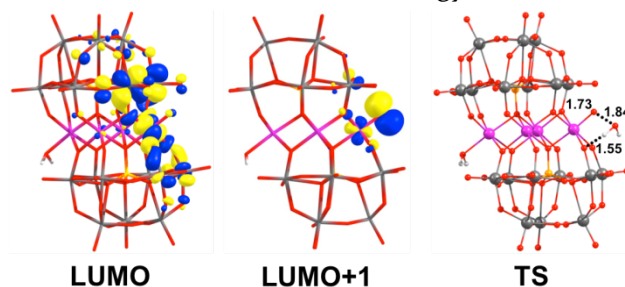


Figure 7. LUMO and LUMO+1 orbital of the $[\text{Co}^{\text{III}}(\text{O}^{\cdot})\text{Co}_3^{\text{II}}(\text{H}_2\text{O})(\text{PW}_9\text{O}_{34})_2]^{10-}$ (S_2) species, as well as transition state structure associated by water nucleophilic attack to $[\text{Co}^{\text{II}}(\text{O})(\text{H}_2\text{O})\text{Co}_3^{\text{II}}(\text{H}_2\text{O})(\text{PW}_9\text{O}_{34})_2]^{10-}$ (TS); distances are given in Å.

One should mention that some of previous studies have proposed the water molecules of solvation shells to be a proton acceptor, but our studies of PCo_4 show that the bridging oxygen of the Co-O-W moiety is the favored proton acceptor,[40, 45, 61-63] similar to the situation proposed in the Ru-substituted Keggin anions.[46]

Thus, above presented data show that PCo_4 -catalyzed water oxidation starts with the sequential ET+PT event $[S_0(\text{Co}^{\text{II}}\text{-OH}_2) \rightarrow S_1' \rightarrow S_1(\text{Co}^{\text{III}}\text{-OH})]$ followed by the formation of the reactive $S_2(\text{Co}^{\text{III}}\text{-O}^{\cdot})$ species via the PCET event $[S_1(\text{Co}^{\text{III}}\text{-OH}) \rightarrow S_2(\text{Co}^{\text{III}}\text{-O}^{\cdot})]$. The $S_2(\text{Co}^{\text{III}}\text{-O}^{\cdot})$ intermediate reacts with an external water molecule then two subsequent PCETs result in the formation of molecular O_2 . In this mechanism, the $S_1(\text{Co}^{\text{III}}\text{-OH}) \rightarrow S_2(\text{Co}^{\text{III}}\text{-O}^{\cdot})$ step determines the potential

required for the formation of the *active species*.^[59] As shown above, the electrochemical generation of the active species $S_2(\text{Co}^{\text{III}}-\text{O}^\bullet)$ formation requires 1.48 V of applied potential at pH=8, which would correspond to an overpotential of 0.72 V. [Note that overpotential (η) is simply the difference between $\Delta G(S_1 \rightarrow S_2)$ and $\Delta G(2\text{H}_2\text{O} \rightarrow \text{O}_2 + 2\text{H}_2)/4$]. As already mentioned, WOC reactions are frequently facilitated photochemically. Formally, electrochemical and photochemical processes are rather similar, but energetic balance requires consideration of the oxi-reduction of the sacrificial electron acceptor.

On the other hand, the kinetics of the chemical O–O bond formation is determined by the O–O bond formation transition state. This reaction step requires an energy of 22.8 kcal·mol⁻¹ (0.99 eV), which is clearly accessible at room temperature when the applied potential is positive enough to shift the pre-equilibria toward the reactive $\text{Co}^{\text{III}}-\text{O}^\bullet$ species (S_2).

Comparison of these findings for PCo_4 catalyst with those for the previously studied Ru^{III} based catalysts (both those in organometallic and POM frameworks) shows that oxidation of Ru centers occurs at lower potentials than Co center. Indeed, the one-electron oxidation potential for $[\text{Ru}^{\text{III}}(\text{H}_2\text{O})\text{SiW}_{11}\text{O}_{39}]^{5-}$ was reported to be 0.64 V vs. SCE (0.88 V vs NHE),^[67] while its computed value was 0.45V.^[46] For the Ru_4 -POM, $[\text{Ru}_4\text{O}_4(\text{OH})_2(\text{H}_2\text{O})_4(\gamma\text{-SiW}_{10}\text{O}_{36})_2]^{10-}$, the PCET event leading to the formation of active $\text{Ru}^{\text{V}}-\text{O}^\bullet$ species is reported to require 1.53 V potential (at pH =0), 400 mV lower than the potential we have found for PCo_4 .^[45] In contrast, the energy for the O–O bond formation was reported to be rather high in $[\text{Ru}^{\text{III}}(\text{H}_2\text{O})\text{SiW}_{11}\text{O}_{39}]^{5-}$ (1.23 eV, 28.4 kcal·mol⁻¹).^[46]

Indeed, it is worth mentioning that TOF values measured for tetraruthenium and PCo_4 anions indicate a higher catalytic activity for PCo_4 suggesting a lower free energy barrier for the latter.^[24]

3. Water oxidation catalyzed by the VCo_4 polyoxometalate. As explained above, the replacement of P^{V} in PCo_4 by V^{V} results in the $[\text{Co}_4(\text{H}_2\text{O})_2(\text{VW}_9\text{O}_{34})_2]^{10-}$ (VCo_4) anion, which exhibits a greater hydrolytic stability than PCo_4 . Furthermore, VCo_4 is a relatively faster water oxidation catalyst than PCo_4 under photochemical conditions.^[60] Such a change in stability and reactivity of the catalyst upon going from PCo_4 to VCo_4 likely reflects the differences in electronic structure of the two POMs, despite the fact that both PCo_4 and VCo_4 have a same overall charge

and nearly identical geometries.^[32, 33, 60] This statement is partly supported by the UV-vis spectra that show transitions involving orbitals of cobalt and heteroatom (vanadium) for VCo_4 , whereas these transitions do not appear for the PCo_4 . This finding indicates involvement of vanadium d orbitals in redox chemistry of VCo_4 .^[60]

In order to provide computational support and elucidate additional factors explaining the difference in stability and reactivity of PCo_4 and VCo_4 systems, we also computed the water oxidation mechanism for the VCo_4 system and compared the resulting data with that for the PCo_4 system.

As reported previously, the calculated geometry and the corresponding X-ray crystallographic values for PCo_4 and VCo_4 are in close agreement. Meanwhile, there exist several remarkable differences (see Table 1) in the calculated energy values of the analogous steps of the PCo_4 - and VCo_4 -catalyzed water oxidation cycles. The most significant differences are in: (a) the increase of the potential for oxidation of Co^{II} -center to the Co^{III} one ($S_0 \rightarrow S_1'$), and (b) the reduction of the energy barrier upon the nucleophilic attack of water on the $\text{Co}^{\text{III}}-\text{oxyl}$ group ($S_2 \rightarrow \text{TS}$). Indeed, the $S_0 \rightarrow S_1'$ transition for VCo_4 requires a 1.58 V of applied potential, which is a 0.31 V larger than that required for PCo_4 . These differences for the PCo_4 and VCo_4 systems could be explained by coupling of d orbitals of V and Co atoms in VCo_4 which results in stabilization of the e_g -type electrons of the $\text{Co}(\text{II})$ center in S_0 state, and increases in oxidation potential of $\text{Co}(\text{II})$ -center to give the low-spin $\text{Co}(\text{III})$ center in S_1' state without e_g -type electrons. This also confers an additional structural stability to VCo_4 during catalytic turnover. Because of the complexity of the systems and the extensive delocalization electrons in canonical orbitals a simple examination of the occupied molecular orbitals in the S_0 state does not permit to identify a unique (or a few number) orbital(s) that recovers the coupling between V and Co orbitals. However, unoccupied orbitals are usually much more localized and thanks to that the V – Co coupling in e_g -type orbitals has been characterized in the parent S_1' species. A detailed description is provided in the SI (Figure S1).

One should emphasize that, although the $\text{Co}^{\text{II}}/\text{Co}^{\text{III}}$ (i.e. $S_0 \rightarrow S_1'$ step) oxidation potential increases upon going from PCo_4 to VCo_4 , this change is not expected to have significant influence to the overall catalytic performance of the Co_4 -POM systems since the step that determines the overpotential ($S_1 \rightarrow S_2$ step) appears later in the catalytic cycle.

Once the species (S_0) with all- Co^{II} centers is oxidized to the species (S_1') with three Co^{II} and one Co^{III} centers, the next two events in the water oxidation cycle do not directly involve the active Co center. As a consequence, the energy required for the following steps is not expected to be dramatically different for the PCo_4 and VCo_4 catalysts. Indeed, our calculations show that: (a) the deprotonation ($S_1' \rightarrow S_1$) requires a slightly higher energy ($7.4 \text{ kcal}\cdot\text{mol}^{-1}$, 0.32 eV) for VCo_4 than for PCo_4 ($5.5 \text{ kcal}\cdot\text{mol}^{-1}$, 0.24 eV); and (2) the second PCET event ($S_1 \rightarrow S_2$) is only $+0.14 \text{ V}$ higher in energy for VCo_4 than for PCo_4 (Table 1).

As outlined above, the following step in the Co_4 -POM-catalyzed water oxidation cycle is O-O bond formation initiated by the nucleophilic attack of external water on the Co^{III} -oxyl group. The computed activation free energy for VCo_4 ($16.8 \text{ kcal}\cdot\text{mol}^{-1}$, 0.73 eV) is about $6 \text{ kcal}\cdot\text{mol}^{-1}$ (0.26 eV) lower than that found for the PCo_4 anion, see Figure 8. Thus, if the active Co^{III} -oxyl intermediate is already formed by various means, such as electrochemical, photo-induced or chemical pathways, then the O-O bond formation is expected to be faster for VCo_4 than for PCo_4 . This conclusion qualitatively agrees with the observed kinetic behavior reported by Hill and co-workers, who have shown that VCo_4 displays faster kinetics than PCo_4 . While the trend is well reproduced, the computed absolute values of the free energy barriers (16.8 and $22.8 \text{ kcal}\cdot\text{mol}^{-1}$ for VCo_4 and PCo_4) are somewhat higher than those estimated from experimental TOFs (13 and $16 \text{ kcal}\cdot\text{mol}^{-1}$, respectively). However, if we consider the overestimation of entropy penalty for these biomolecular processes, the calculations are in reasonable good agreement with observations (see Table S5 in the Supporting Information). All these results are consistent with the fact that the O-O bond formation step might be the turnover-limiting chemical step, after the formation of the catalytic active Co^{III} -oxyl intermediate.[73]

In order to elucidate reason of the aforementioned reduction of the O-O bond formation barrier upon going from PCo_4 to VCo_4 , we analyzed a set of lowest unoccupied orbitals of their S_2 species, because these could be the acceptor orbitals in the nucleophilic attack of water. For PCo_4 , we found that LUMO and LUMO+1 orbitals have -2.88 eV and -2.75 eV energies, respectively. Among these orbitals, the LUMO+1 has a strong p(oxyl) contribution and, therefore, is the best candidate to accept electrons from the coordinated water molecule (see Figure 7). However, in the case of VCo_4 , three unoccupied orbitals, namely, LUMO, LUMO+1 and LUMO+2 orbitals, have a strong contribution from the oxyl

oxygen (Figure 9) and are good candidates for being an acceptor orbitals. Interestingly, all these three orbitals are lie lower in energy (at the positions of -2.95 eV , -2.78 eV and -2.77 eV , respectively) than the LUMO and LUMO+1 orbitals of the S_2 species of PCo_4 . Therefore, one may expect attack of water molecule to the S_2 species to be more favorable for VCo_4 than for PCo_4 .

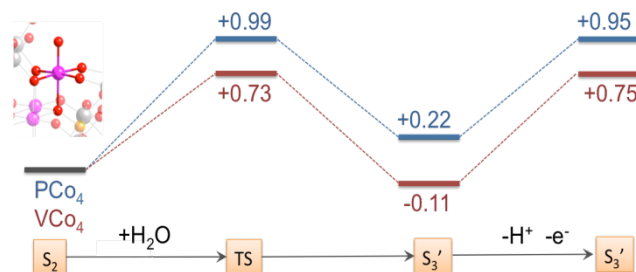


Figure 8. Energy profile corresponding to the water nucleophilic attack to Co^{III} -oxyl species (S_2), and subsequent PCET event started from protonated Co^{II} -OOH POM (S_3') (energies are in eV).

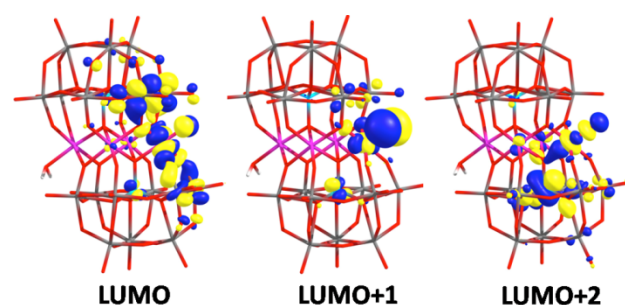


Figure 9. LUMO, LUMO+1 and LUMO+2 orbitals of the $[\text{Co}^{\text{III}}(\text{O})\text{Co}_3^{\text{II}}(\text{H}_2\text{O})(\text{VW}_9\text{O}_{34})_2]^{10-}$ (S_2) species.

CONCLUSIONS

From the above present computational studies we may conclude:

1. The initial H-atom removal step [$S_0(\text{POM-Co}^{\text{II}}-\text{OH}_2) \rightarrow S_1(\text{POM-Co}^{\text{III}}-\text{OH})$] in water oxidation catalyzed by the PCo_4 and VCo_4 anions could proceed via the uncoupled electron-then-proton transfer (ET+PT) pathway and leads to one-electron oxidize species S_1 . Although we cannot discard the concerted PCET event being competitive with the ET+PT pathway when the applied potential is held high enough, since both processes are relatively close in energy. The second H-atom removal from the OH-fragment of S_1 is a concerted PCET event and forms the Co^{III} -O \cdot active species S_2 . The overall $S_0 \rightarrow S_2$ transformation is estimated to require less than 1.48 V and 1.62 V at $\text{pH}=8$ for PCo_4 and VCo_4 anions, respectively, which determine the overpotential for the overall catalytic reaction.[59]
2. The O-H bond cleavage (i.e. $S_1' \rightarrow S_1$ step) together with the O-O bond formation, i.e. the

chemical steps of the reaction, control the kinetics of the reaction. Where the O–O bond formation occurs via a “water nucleophilic attack” mechanism from the Co^{III}-oxyl intermediate **S**₂, which requires 22.8 kcal·mol⁻¹ (0.99 eV) and 16.8 kcal·mol⁻¹ (0.73 eV) energy barriers for **PCo**₄ and **VCo**₄, respectively.

- Comparison of the calculated energetics for the **PCo**₄ and **VCo**₄ anions shows that coupling of d orbitals of V and Co atoms in **VCo**₄ results in stabilization of high-spin Co(II)-centers with e_g-type electrons compared to the low-spin Co(III)-centers. Orbital coupling is also predicted to be reason (or one of reasons) for observed enhancement of catalytic activity of **VCo**₄ compared to **PCo**₄.

In summary, using a relatively simple model system we have been able to propose a plausible reaction mechanism for Co-containing POM acting as WOCs. We are convinced that in the years to come the combination of additional experimental data with more sophisticated models that consider, for example, the effect of the buffer, ionic strength, or the incorporation of explicit waters in some steps will allow to advance further in understanding of these complex catalytic reactions.

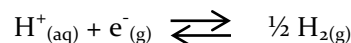
Computational Details. All reported calculations were performed with the Gaussian-09 package[74] at density functional theory (DFT) level by utilizing B3LYP functional.[75-77] Recently, Fabris *et al.* have shown that exchange-correlation hybrid functionals such as the B3LYP and the PBE0 lead to a fair agreement with the coupled cluster energies for the water oxidation process by cobalt oxide clusters.[78] In fact, latter successful computational studies on WOC process by Co systems employed B3LYP functional.[56, 58] This latter functional has been widely used in theoretical studies of TM substituted polyoxometalates.[72],[79-82]

For P, Co and W atoms, the LANL2DZ effective core potential (ECP) and associated basis sets were used.[83] The 6-31G(d,p) basis set was used for O atoms directly bound to Co and the 6-31G basis set for the rest of atoms.[84-86] All the structures were optimized in water using IEF-PCM approach to model the solvent effects ($\epsilon = 78.36$ and UFF radii). [87] The nature of all stationary points was verified by vibrational frequencies, which were also used for calculation of free energy contributions. A data set collection of computational results is available in the ioChem-BD repository[88] and can be accessed via doi:10.19061/iochem-bd-2-6.

In order to investigate the energies required to reach each step in the catalytic cycle we adopted the energetic scheme proposed by Voorhis:[43]

$$E^0 = \frac{1}{F} (\Delta G_{(g)}^0 + \Delta G_{solv} - n_{H^+} G_{(aq)}^{0H^+}) - 4.24V \quad (1)$$

where F is the Faraday constant, $\Delta G_{(g)}^0$ is the free energy change associated with oxidation in vacuum, ΔG_{solv} is the free energy of solvation, $G_{(aq)}^{0H^+}$ is the standard free energy of a proton in aqueous solution for which we adopted a value of -11.803 eV, the negative term ($E_{abs}^* = -4.24$ V) is the absolute standard potential of the half-reaction:



For elementary electrochemical steps that involve a proton transfer, the measured potential at experimental pH conditions is related to standard conditions (pH=0) by the Nernst equation that at a room temperature is (in V)

$$E = E^0 - 0.059 * pH \quad (2)$$

Calculated pK_a values were obtained from the free energy of deprotonation steps using the standard equation:[89, 90]

$$pK_a = -\log_{10} e^{-\Delta G_{a(s)}/RT} \quad (3)$$

ASSOCIATED CONTENT

Supporting Information. Electronic and free energies, configurations, charges, and multiplicities, as well as atomic spin densities, and cartesian coordinates of all the computed structures of the catalytic cycle.

AUTHOR INFORMATION

Corresponding Author

* josepmaria.poblet@urv.cat; j.carbo@urv.cat; dmusaev@emory.edu

Author Contributions

All authors have given approval to the final version of the manuscript.

ACKNOWLEDGMENT

We thank the Spanish Ministry of Science and Innovation (grant CTQ2014-52774-P), the DGR of the Generalitat de Catalunya (grant 2014SGR199 and XRQTC). We thank also CMST COST Action CM1203. J.M.P. thanks ICREA foundation for an ICREA ACADEMIA award for research excellence. D.G.M. and C.L.H. are acknowledging U.S. Department of Energy, Office of Basic Energy Sciences, Solar Photochemistry Program (DE-FG02-07ER-15906) for support, as well as NSF MRI-R2 grant (CHE-0958205) and the use of the resources of the Cherry Emerson Center for Scientific Computation. We are very grateful to referees for their helpful comments.

REFERENCES

- [1] N.S. Lewis, D.G. Nocera, *Proc. Natl. Acad. Sci.*, 103 (2006) 15729–15735.
- [2] V. Balzani, A. Credi, M. Venturi, *ChemSusChem*, 1 (2008) 26–58.
- [3] H. Dau, C. Limberg, T. Reier, M. Risch, S. Roggan, P. Strasser, *ChemCatChem*, 2 (2010) 724–761.
- [4] X. Liu, F.Y. Wang, *Coord. Chem. Rev.*, 256 (2012) 1115–1136.
- [5] D.J. Wasylenko, R.D. Palmer, C.P. Berlinguette, *Chem. Commun.*, 49 (2013) 218–227.
- [6] J.J. Concepcion, J.W. Jurss, M.K. Brennaman, P.G. Hoertz, A.O.T. Patrocínio, N.Y. Murakami Iha, J.L. Templeton, T.J. Meyer, *Acc. Chem. Res.*, 42 (2009) 1954–1965.
- [7] Y. Jiang, F. Li, B. Zhang, X. Li, X. Wang, F. Huang, L. Sun, *Angew. Chem. Int. Ed.*, 52 (2013) 3398–3401.
- [8] J.D. Blakemore, N.D. Schley, D. Balcells, J.F. Hull, G.W. Olack, C.D. Incarvito, O. Eisenstein, G.W. Brudvig, R.H. Crabtree, *J. Am. Chem. Soc.*, 132 (2010) 16017–16029.
- [9] L. Duan, F. Bozoglian, S. Mandal, B. Stewart, T. Privalov, A. Llobet, L. Sun, *Nat. Chem.*, 4 (2012) 418–423.
- [10] J. Lloret-Fillol, Z. Codolà, I. Garcia-Bosch, L. Gómez, J.J. Pla, M. Costas, *Nat. Chem.*, 3 (2011) 807–813.
- [11] R. Lalrempuia, N.D. McDaniel, H. Müller-Bunz, S. Bernhard, M. Albrecht, *Angew. Chem. Int. Ed.*, 49 (2010) 9765–9768.
- [12] S.M. Barnett, K.I. Goldberg, J.M. Mayer, *Nat. Chem.*, 4 (2012) 498–502.
- [13] D.J. Wasylenko, C. Ganesamoorthy, J. Borau-Garcia, C.P. Berlinguette, *Chem. Commun.*, 47 (2011) 4249–4251.
- [14] N.S. McCool, D.M. Robinson, J.E. Sheats, G.C. Dismukes, *J. Am. Chem. Soc.*, 133 (2011) 11446–11449.
- [15] M.-T. Zhang, Z. Chen, P. Kang, T.J. Meyer, *J. Am. Chem. Soc.*, 135 (2013) 2048–4051.
- [16] C. Sens, I. Romero, M. Rodríguez, A. Llobet, T. Parella, J. Benet-Cuchholz, *J. Am. Chem. Soc.*, 126 (2004) 7798–7799.
- [17] F. Bozoglian, S. Romain, M.Z. Ertem, T.K. Todorova, C. Sens, J. Mola, M. Rodríguez, I. Romero, J. Benet-Buchholz, X. Fontrodona, C.J. Cramer, L. Gagliardi, A. Llobet, *J. Am. Chem. Soc.*, 131 (2009) 15176–15187.
- [18] J.J. Concepcion, J.W. Jurss, J.L. Templeton, T.J. Meyer, *J. Am. Chem. Soc.*, 130 (2008) 16462–16463.
- [19] Y. Xu, A. Fischer, L. Duan, L. Tong, E. Gabrielsson, B. Åkermark, L. Sun, *Angew. Chem. Int. Ed.*, 49 (2010) 8934–8937.
- [20] M.T. Pope, A. Müller, *Polyoxometalate Chemistry: From Topology via self-Assembly to Applications*, Springer, New York, 2001.
- [21] L. Cronin, A. Müller, *Chem. Soc. Rev.*, 41 (2012) 7333–7334.
- [22] J.J. Stracke, R.G. Finke, *ACS Catal.*, 4 (2014) 909–933.
- [23] R. Schiwon, K. Klingan, H. Dau, C. Limberg, *Chem. Commun.*, 50 (2013) 100–102.
- [24] H. Lv, Y.V. Geletii, C. Zhao, J.W. Vickers, G. Zhu, Z. Luo, J. Song, T. Lian, D.J. Musaev, C.L. Hill, *Chem. Soc. Rev.*, 41 (2012) 7572–7589.
- [25] S. Goberna-Ferrón, J. Soriano-López, J.R. Galán-Mascarós, M. Nyman, *Eur. J. Inorg. Chem.*, 2015 (2015) 2833–2840.
- [26] A. Sartorel, M. Carraro, G. Scorrano, R. De Zorzi, S. Geremia, N.D. McDaniel, S. Bernhard, M. Bonchio, *J. Am. Chem. Soc.*, 130 (2008) 5006–5007.
- [27] A. Sartorel, P. Miró, E. Salvarodi, S. Romain, M. Carraro, G. Scorrano, M. Di Valentin, A. Llobet, C. Bo, M. Bonchio, *J. Am. Chem. Soc.*, 131 (2009) 16051–16053.
- [28] F.M. Toma, A. Sartorel, M. Iurlo, M. Carraro, P. Parrisè, C. Maccato, S. Rapino, B. Rodriguez-Gonzalez, H. Amenitsch, T. Da

- Ros, L. Casalis, A. Goldoni, M. Marcaccio, G. Scorrano, G. Scoles, F. Paolucci, M. Prato, M. Bonchio, *Nat. Chem.*, 2 (2010) 826–831.
- [29] Y.V. Geletii, B. Botar, P. Koegerler, D.A. Hillesheim, D.G. Musaev, C.L. Hill, *Angew. Chem. Int. Ed.*, 47 (2008) 3896–3899.
- [30] Y.V. Geletii, Z. Huang, Y. Hou, D.G. Musaev, T. Lian, C.L. Hill, *J. Am. Chem. Soc.*, 131 (2009) 7522–7523.
- [31] C. Besson, Z. Huang, Y.V. Geletii, S. Lense, K.I. Hardcastle, D.G. Musaev, T. Lian, A. Proust, C.L. Hill, *Chem. Commun.*, 46 (2010) 2784–2786.
- [32] Q. Yin, J.M. Tan, C. Besson, Y.V. Geletii, D.G. Musaev, A.E. Kuznetsov, Z. Luo, K.I. Hardcastle, C.L. Hill, *Science*, 328 (2010) 342–345.
- [33] J.W. Vickers, H. Lv, M. Sumliner, G. Zhu, Z. Luo, D.G. Musaev, Y.V. Geletii, C.L. Hill, *J. Am. Chem. Soc.*, 135 (2013) 14110–14118.
- [34] S. Goberna-Ferrón, L. Vígara, J. Soriano-López, J.R. Galán-Mascarós, *Inorg. Chem.*, 51 (2012) 11707–11715.
- [35] J. Soriano-López, S. Goberna-Ferrón, L. Vígara, J.J. Carbó, J.M. Poblet, J.R. Galán-Mascarós, *Inorg. Chem.*, 52 (2013) 4753–4755.
- [36] M.W. Kanan, D.G. Nocera, *Science*, 321 (2008) 1072–1075.
- [37] S. Goberna-Ferrón, B. Peña, J. Soriano-López, J.J. Carbó, H. Zhao, J.M. Poblet, K.R. Dunbar, J.R. Galán-Mascarós, *J. Catal.*, 315 (2014) 25–32.
- [38] R. Kang, K. Chen, J. Yao, S. Shaik, H. Chen, *Inorg. Chem.*, 53 (2014) 7130–7136.
- [39] M. Hirahara, M.Z. Ertem, M. Komji, H. Yamazaki, C.J. Cramer, M. Yagi, *Inorg. Chem.*, 52 (2013) 6354–6364.
- [40] L. Vígara, M.Z. Ertem, N. Planas, F. Bozoglian, N. Leidel, H. Dau, M. Haumann, L. Gagliardi, C.J. Cramer, A. Llobet, *Chem. Sci.*, 3 (2012) 2576–2586.
- [41] S. Roeser, M.Z. Ertem, C. Cady, R. Lomoth, J. Benet-Buchholz, L. Hammarström, B. Sarkar, W. Kaim, C.J. Cramer, A. Llobet, *Inorg. Chem.*, 51 (2012) 320–327.
- [42] J.J. Concepcion, M.-K. Tsai, J.T. Muckerman, T.J. Meyer, *J. Am. Chem. Soc.*, 132 (2010) 1545–1557.
- [43] L.-P. Wang, Q. Wu, T. Van Voorhis, *Inorg. Chem.*, 49 (2010) 4543–4553.
- [44] X. Sala, M.Z. Ertem, L. Vígara, T.K. Todorova, W. Chen, R. C., R.C. Rocha, F. Aquilante, C.J. Cramer, L. Gagliardi, A. Llobet, *Angew. Chem. Int. Ed.*, 49 (2010) 7745–7747.
- [45] S. Piccinin, A. Sartorel, G. Aquilanti, A. Goldoni, M. Bonchio, S. Fabris, *Proc. Natl. Acad. Sci.*, 110 (2013) 4917–4922.
- [46] L. Z-L., G.-C. Yang, N.-N. Ma, S.-Z. Wen, L.-K. Yan, W. Guan, Z.-M. Su, *Dalton. Trans.*, 42 (2013) 10617–10625.
- [47] S. Piccinin, S. Fabris, *Phys. Chem. Chem. Phys.*, 13 (2011) 7666–7674.
- [48] A.E. Kuznetsov, Y.V. Geletii, C.L. Hill, K. Morokuma, D.G. Musaev, *Theor. Chem. Acc.*, 130 (2011) 197–207.
- [49] D. Quiñonero, A.L. Kaledin, A.E. Kuznetsov, Y.V. Geletii, C. Besson, C.L. Hill, D.G. Musaev, *J. Phys. Chem. A*, 114 (2010) 535–542.
- [50] A.E. Kuznetsov, Y.V. Geletii, C.L. Hill, K. Morokuma, D.G. Musaev, *J. Am. Chem. Soc.*, 131 (2009) 6844–6854.
- [51] S. Piccinin, S. Fabris, *Inorganics*, 3 (2015) 374–387.
- [52] L.-P. Wang, T. Van Voorhis, *J. Phys. Chem. Lett.*, 2 (2011) 2200–2204.
- [53] X. Li, P.E.M. Siegbahn, *J. Am. Chem. Soc.*, 135 (2013) 13804–13813.
- [54] J.G. McAlpin, T.A. Stich, C.A. Ohlin, Y. Surendranath, D.G. Nocera, W.H. Casey, R.D. Britt, *J. Am. Chem. Soc.*, 133 (2011) 15444–15452.

- [55] G. Mattioli, P. Giannozzi, A.A. Bonapasta, L. Guidoni, *J. Am. Chem. Soc.*, **135** (2013) 15353–15363.
- [56] A. Fernando, C.M. Aikens, *J. Phys. Chem.*, **119** (2015) 11072–11085.
- [57] M. Bajdich, M. García-Mota, A. Vojvodic, J.K. Nørskov, A.T. Bell, *J. Am. Chem. Soc.*, **135** (2013) 13521–13530.
- [58] F.H. Hodel, S. Lubner, *ACS Catal.*, **6** (2016) 1505–1517.
- [59] M.G. Mavros, T. Tsuchimochi, T. Kowalczyk, A. Mclssac, L.-P. Wang, T. Van Voorhis, *Inorg. Chem.*, **53** (2014) 6386–6397.
- [60] H. Lv, J. Song, Y.V. Geletii, J.W. Vickers, J.M. Sumliner, D.G. Musaev, P. Koegerler, P.F. Zhuk, J. Bacsa, G. Zhu, C.L. Hill, *J. Am. Chem. Soc.*, **136** (2014) 9268–9271.
- [61] H. Lei, A. Han, F. Li, M. Zhang, Y. Han, P. Du, W. Lai, R. Cao, *Phys. Chem. Chem. Phys.*, **16** (2014) 1883–1893.
- [62] W. Lai, R. Cao, G. Dong, S. Shaik, J. Yao, H. Chen, *J. Phys. Chem. Lett.*, **3** (2012) 2315–2319.
- [63] M.Z. Ertem, C.J. Cramer, *Dalton. Trans.*, **41** (2012) 12213–12219.
- [64] C.A. Ohlin, S.J. Harley, J.G. McAlpin, R.K. Hocking, B.Q. Mercado, R.L. Johnson, E.M. Villa, M.K. Fidler, M.M. Olmstead, L. Spiccia, R.D. Britt, W.H. Casey, *Chem. Eur. J.*, **17** (2011) 4408–4417.
- [65] D. Lieb, A. Zahl, E.F. Wilson, C. Streb, L.C. Nye, K. Meyer, I. Ivanović-Burmazović, *Inorg. Chem.*, **50** (2011) 9053–9058.
- [66] J.J. Stracke, R.G. Finke, *ACS Catal.*, **3** (2013) 1209–1219.
- [67] M. Murakami, D. Hong, T. Suenobu, S. Yamaguchi, T. Ogura, S. Fukuzumi, *J. Am. Chem. Soc.*, **133** (2011) 11605–11613.
- [68] D. Barats-Damatov, L.J.W. Shimon, L. Weiner, R.E. Schreiber, P. Jiménez-Lozano, J.M. Poblet, C. de Graaf, R. Neumann, *Inorg. Chem.*, **53** (2014) 1779–1787.
- [69] P. Jiménez-Lozano, J.J. Carbó, A. Chaumont, J.M. Poblet, A. Rodríguez-Forteza, G. Wipff, *Inorg. Chem.*, **53** (2014) 778–786.
- [70] P. Jiménez-Lozano, I.D. Ivanchikova, O.A. Kholdeeva, J.M. Poblet, J.J. Carbó, *Chem. Commun.*, **48** (2012) 9266–9268.
- [71] X. López, I.A. Weinstock, C. Bo, J.P. Sarasa, J.M. Poblet, *Inorg. Chem.*, **45** (2006) 6467–6473.
- [72] X. López, J.J. Carbo, C. Bo, J.M. Poblet, *Chem. Soc. Rev.*, **41** (2012) 7537–7571.
- [73] Y. Surendranath, M.W. Kanan, D.G. Nocera, *J. Am. Chem. Soc.*, **132** (2010) 16501–16509.
- [74] M.J. Frisch, G.W. Trucks, H.B. Schlegel, G.E. Scuseria, M.A. Robb, J.R. Cheeseman, G. Scalmani, V. Barone, B. Mennucci, G.A. Petersson, H. Nakatsuji, M. Caricato, X. Li, H.P. Hratchian, A.F. Izmaylov, J. Bloino, G. Zheng, J.L. Sonnenberg, M. Hada, M. Ehara, K. Toyota, R. Fukuda, J. Hasegawa, M. Ishida, T. Nakajima, Y. Honda, O. Kitao, H. Nakai, T. Vreven, J.A. Montgomery, J.E. Peralta, F. Ogliaro, M. Bearpark, J.J. Heyd, E. Brothers, K.N. Kudin, V.N. Staroverov, R. Kobayashi, J. Normand, K. Raghavachari, A. Rendell, J.C. Burant, S.S. Iyengar, J. Tomasi, M. Cossi, N. Rega, J.M. Millam, M. Klene, J.E. Knox, J.B. Cross, V. Bakken, C. Adamo, J. Jaramillo, R. Gomperts, R.E. Stratmann, O. Yazyev, A.J. Austin, R. Cammi, C. Pomelli, J.W. Ochterski, R.L. Martin, K. Morokuma, V.G. Zakrzewski, G.A. Voth, P. Salvador, J.J. Dannenberg, S. Dapprich, A.D. Daniels, Farkas, J.B. Foresman, J.V. Ortiz, J. Cioslowski, D.J. Fox, *Gaussian 09*, Revision C.01, in, Wallingford CT, 2010.
- [75] C. Lee, C. Yang, R.G. Parr, *Phys. Rev. B*, **38** (1988) 785–789.
- [76] A.D. Becke, *J. Chem. Phys.*, **98** (1993) 5648–5652.
- [77] P.J. Stephens, F.J. Devlin, C.F. Chabalowski, M.J. Frisch, *J. Phys. Chem.*, **98** (1994) 11623–11627.
- [78] K. Kwapien, S. Piccinin, S. Fabris, *J. Phys. Chem. Lett.*, **4** (2013) 4223–4230.
- [79] K. Nishiki, N. Umehara, Y. Kadota, X. López, J.M. Poblet, C.A. Mezui, A.-L. Teillout, I.M. Mbomekalle, P.d. Oliveira, M.

- Miyamoto, T. Sanoa, M. Sadakane, Dalton Trans., 45 (2016) 3175–3726.
- [80] P.A. Aparicio, J.M. Poblet, X. López, Eur. J. Inorg. Chem., (2013) 1910–1916.
- [81] P. Jiménez-Lozano, I.Y. Skobelev, O.A. Kholdeeva, J.M. Poblet, J.J. Carbó, Inorg. Chem., (2016) 6080–6084.
- [82] C. Ci, J.J. Carbó, R. Neumann, C.d. Graaf, J.M. Poblet, ACS Catal., (2016) 6422–6428.
- [83] P.J. Hay, W.R. Wadt, J. Chem. Phys., 82 (1985) 270–283.
- [84] M.M. Francl, W.J. Pietro, W.J. Hehre, J.S. Binkley, M.S. Gordon, D.J. Defrees, J.A. Pople, J. Chem. Phys., 77 (1982) 3654–3665.
- [85] W.J. Hehre, R. Ditchfield, J.A. Pople, J. Chem. Phys., 56 (1972) 2257–2261.
- [86] P.C. Hariharan, J.A. Pople, Theor. Chim. Acta, 25 (1973) 213–222.
- [87] E. Cancès, B. Mennucci, J. Tomasi, J. Chem. Phys., 107 (1997) 3032–3041.
- [88] M. Álvarez-Moreno, C. de Graaf, N. Lopez, F. Maseras, J.M. Poblet, C. Bo, J. Chem. Inf. Model., 55 (2015) 95–103.
- [89] J. Li, C.L. Fisher, J.L. Chen, D. Bashford, L. Noodleman, Inorg. Chem., 35 (1996) 4694–4702.
- [90] J.R. Buchwald, S. Kal, P.H. Dinolfo, J. Phys. Chem. C, 118 (2014) 25869–25877.